The EMBO Journal (2006) 25, 1590–1602 | © 2006 European Molecular Biology Organization | All Rights Reserved 0261-4189/06
www.embojournal.org

THE EMBO JOURNAL

GGA function is required for maturation of neuroendocrine secretory granules

Or Kakhlon[1], Prabhat Sakya[2], Banafshe Larijani[2], Rose Watson[3] and Sharon A Tooze[1,*]

[1]Secretory Pathway Laboratories, Cancer Research UK, London Research Institute, London, UK, [2]Cell Biophysics, Cancer Research UK, London Research Institute, London, UK and [3]Electron Microscopy Laboratories, Cancer Research UK, London Research Institute, London, UK

Secretory granule (SG) maturation has been proposed to involve formation of clathrin-coated vesicles (CCVs) from immature SGs (ISGs). We tested the effect of inhibiting CCV budding by using the clathrin adaptor GGA (Golgi-associated, γ-ear-containing, ADP-ribosylation factor-binding protein) on SG maturation in neuroendocrine cells. Overexpression of a truncated, GFP-tagged GGA, VHS (Vps27, Hrs, Stam)-GAT (GGA and target of myb (TOM))-GFP led to retention of MPR, VAMP4, and syntaxin 6 in mature SGs (MSGs), suggesting that CCV budding from ISGs is inhibited by the SG-localizing VHS-GAT-GFP. Furthermore, VHS-GAT-GFP-overexpression disrupts prohormone convertase 2 (PC2) autocatalytic cleavage, processing of secretogranin II to its product p18, and the correlation between PC2 and p18 levels. All these effects were not observed if full-length GGA1-GFP was overexpressed. Neither GGA1-GFP nor VHS-GAT-GFP perturbed SG protein budding from the TGN, or homotypic fusion of ISGs. Reducing GGA3 levels by using short interfering (si)RNA also led to VAMP4 retention in SGs, and inhibition of PC2 activity. Our results suggest that inhibition of CCV budding from ISGs downregulates the sorting from the ISGs and perturbs the intragranular activity of PC2.

The EMBO Journal (2006) **25,** 1590–1602. doi:10.1038/sj.emboj.7601067; Published online 6 April 2006
Subject Categories: membranes & transport
Keywords: clathrin-coated vesicles; GGA; granule maturation; secretory granules

Introduction

GGAs (Golgi-associated, γ-ear-containing, ADP-ribosylation factor-binding proteins) are a family of monomeric clathrin adaptors, which facilitate sorting of MPR, and possibly other cargo such as sortilin, into clathrin-coated vesicles (CCVs) (Hirst *et al*, 2000; Nielsen *et al*, 2001; Bonifacino, 2004). All GGAs consist of three domains: VHS (Vps27, Hrs, Stam), which recognizes the cargo acidic-dileucine sorting signal DXXLL; GAT (GGA and target of myb (TOM)), which interacts with GTP-bound ARF; and GAE (γ-adaptin ear), which interacts with accessory proteins such as γ-synergin (Page, 1999, no. 1842) and rabaptin 5 (Hirst *et al*, 2000; Shiba *et al*, 2002; Mattera *et al*, 2003) in mammals, and epsin-related proteins in *Saccharomyces cerevisiae* (Duncan *et al*, 2003). The GAT and GAE domains are connected by a hinge that engages clathrin (Costaguta *et al*, 2001; Mullins and Bonifacino, 2001; Puertollano *et al*, 2001b; Zhu *et al*, 2001) and γ-adaptin (Doray *et al*, 2002).

GGAs do not constitute a stoichiometric constituent of CCVs (Hirst, 2000, no. 2022) and are probably involved in a kinetic proofreading mechanism responsible for the transient retention of AP-1 on membranes and presentation of MPR to AP-1. The former is brought about by GGA displacing ARF-GAP from ARF (Puertollano *et al*, 2001b; Jacques *et al*, 2002), whereas the latter is executed by consecutive phosphoregulatory events in which GGAs are activated (Ghosh and Kornfeld, 2003), 'handed off' from ARF to MPR (Hirsch *et al*, 2003), and then released from MPR, which now has increased avidity for AP-1(Doray *et al*, 2002; Ghosh and Kornfeld, 2003). GGA1 has also been suggested to regulate postbudding dissociation of the clathrin coat (McKay and Kahn, 2004).

One role of GGAs is to package MPRs and their bound hydrolase precursors into CCVs that bud from the TGN and delivered to endosomes. However, GGAs could also function in the formation of carriers from membranes other than the TGN. This notion is supported by the presence of GGAs not only on the TGN but also on peripheral structures (Dell'Angelica *et al*, 2000), endosomes (Puertollano and Bonifacino, 2004), and TGN-derived carriers (Puertollano *et al*, 2003). In this study, we propose a novel target for GGAs—the immature secretory granule (ISGs). ISGs are carriers of regulated secretory proteins that bud from the TGN in neuroendocrine and endocrine cells (Arvan and Castle, 1998; Tooze, 1998), and then mature through homotypic fusion (confirmed only for PC12 cells; Urbé *et al*, 1998) and remodeling of their membrane. This remodeling consists of sorting away a specific set of proteins such as furin (Dittié *et al*, 1997), carboxypeptidase D (Varlamov *et al*, 1999), MPR (Kuliawat *et al*, 1997; Klumperman *et al*, 1998), and the SNAREs' syntaxin 6 (Sx6) (Klumperman *et al*, 1998; Wendler *et al*, 2001) and VAMP4 (Eaton *et al*, 2000; Hinners *et al*, 2003), from maturing ISGs. This sorting depends on recruitment of AP-1 by furin, MPR, and VAMP4 in a phosphorylation-dependent manner (Dittié *et al*, 1997, 1999; Hinners *et al*, 2003). On the basis of the presence of clathrin coats on ISGs and their absence from mature SGs (MSGs), it was proposed that CCVs bud from ISGs during their maturation and are the means by which the ISG membrane is remodeled (Orci *et al*, 1985; Tooze and Tooze, 1986). Two lines of evidence led us to test GGA's involvement in ISG membrane remodeling via CCV budding: (1) ARF1 is found

*Corresponding author. Secretory Pathway Laboratories, Cancer Research UK, London Research Institute, 44 Lincoln's Inn Fields, London WC2A 3PX, UK. Tel.: +44 207 269 3122; Fax: +44 207 269 3417; E-mail: sharon.tooze@cancer.org.uk

Received: 6 October 2005; accepted: 8 March 2006; published online: 6 April 2006

on ISGs, where it recruits AP-1, and not on MSGs (Dittié *et al*, 1996; Austin *et al*, 2000); (2) clathrin coats on ISGs contain AP-1 and MPR (Klumperman *et al*, 1998).

We opted for functional repression of GGA to ask whether GGA regulates CCV budding from ISG and whether this budding plays a significant role in ISG maturation. We used a dominant-negative (DN) form of GGA1 lacking the hinge and GAE domains (VHS-GAT-GFP), which does not recruit clathrin and AP-1, and thus inhibits coat assembly. This strategy was used successfully to inhibit budding of MPR-associated carriers from the TGN (Puertollano *et al*, 2001a, b) and translocation of glucose transporter 4 (Glut4) vesicles from a Glut4 storage compartment (Watson *et al*, 2004). As another approach for repressing GGA, we used short interfering (si)RNA specific for GGA3 (Ghosh *et al*, 2003; Puertollano and Bonifacino, 2004).

Our results show that inhibition of GGAs results in the retention of MPR, and the CCV cargos VAMP4 and Sx6 in SGs. Interestingly, ISG-localized VHS-GAT or siRNA depletion also inhibits maturation of the granules *per se*, by interfering with the processing of secretogranin II (SgII) to p18. Budding from the TGN, or fusiogenicity of the ISGs, was not affected by VHS-GAT. We conclude that GGAs are involved in SG membrane remodeling, and propose that CCV budding is required for efficient SG maturation.

Results

VHS-GAT-GFP functions as a DN GGA and is recruited to ISGs

VHS-GAT is a DN GGA as it blocked budding from the TGN in HeLa cells (Puertollano *et al*, 2001a, b) and in 3T3 L1 adipocytes (Watson *et al*, 2004). Therefore, to confirm that in rat neuroendocrine PC12 cells, VHS-GAT-GFP behaves as a DN GGA, we examined MPR and AP1 distribution in PC12 cells expressing VHS-GAT-GFP or full-length GGA1-GFP. As seen in Figure 1A–H, in VHS-GAT-GFP but not in GGA1-GFP-expressing cells, MPR accumulated at a juxtanuclear area, suggesting that it failed to be recruited into carriers budding from the TGN. AP1, on the other hand, was displaced from membranes in VHS-GAT-GFP-overexpressing cells (Figure 1I–N), indicating competition with ARF1 binding sites, or a

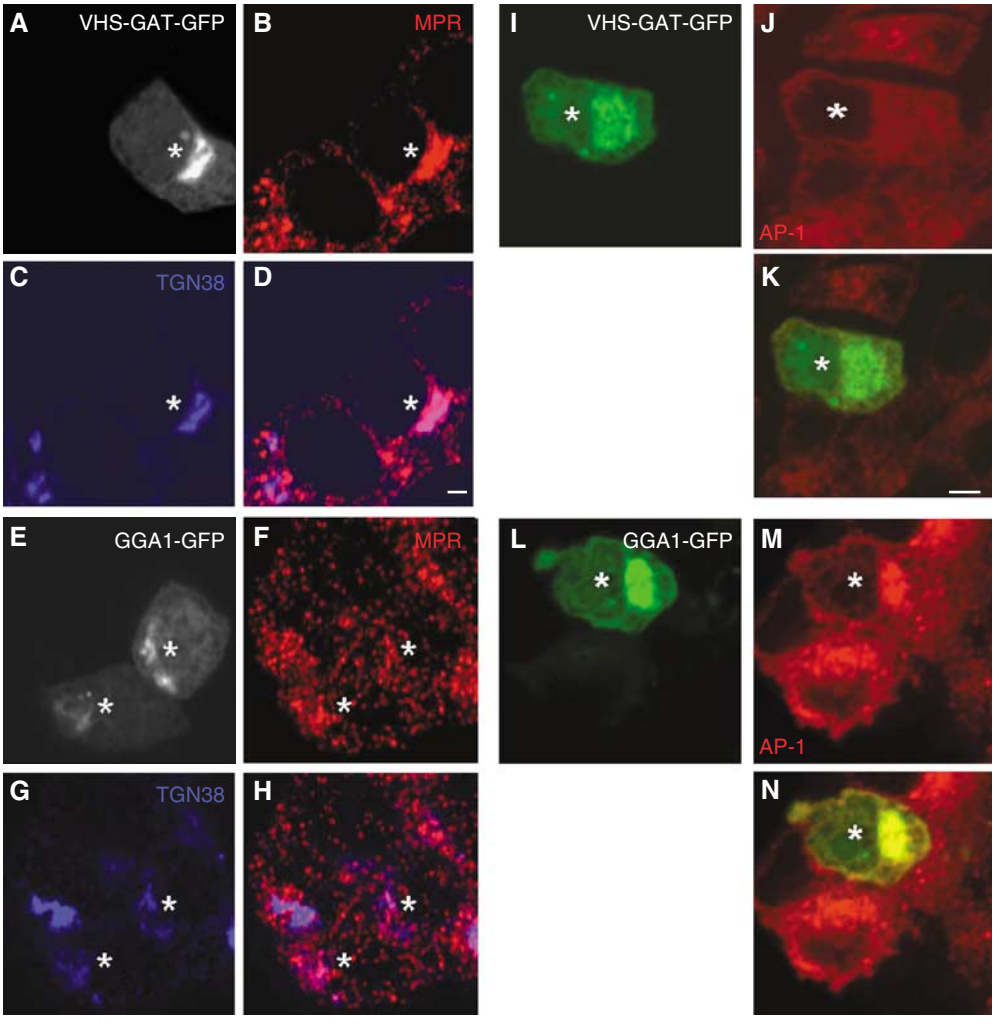

Figure 1 VHS-GAT-GFP but not GGA1-GFP accumulate MPR at a juxtanuclear region and redistribute AP1 to the cytosol. PC12 cells transfected with VHS-GAT-GFP (**A–D, I–J**) or GGA1-GFP (**E–H, L–N**) were fixed 24 h post-transfection and labeled with (B, F) anti-MPR, anti-γ AP (J, M) Abs (red), or (C, G) anti-TGN38 (blue), and secondary Abs. Representative confocal images with the VHS-GAT-GFP (A, I) and GGA1-GFP (E, L) channels are shown. (D), (H), (**K**), and (N) are merged channels of (B) and (C, F and G, I and J, and L and M), respectively. MPR accumulation and AP1 redistribution can be observed in the VHS-GAT-GFP transfected cells (*). Bars = 2 μm.

shortening of AP1 membrane residence time by competing for its interaction with the GGA hinge domain.

To test if GGAs are involved in the maturation of ISGs, we showed that the VHS-GAT-GFP localized to ISG membranes. Figure 2A shows that VHS-GAT-GFP partially localizes to a structure positive for SgII, which is not the TGN, and which we conclude as SGs because SgII is exclusively targeted to SGs. This observation was also corroborated by biochemical data: a postnuclear supernatant (PNS) from PC12 cells transfected with VHS-GAT-GFP was fractionated on velocity gradients (VG) to separate ISGs and MSGs from TGN. Pooled VG fractions 2–4 and 5–7, containing ISGs and MSGs, respectively (Dittié *et al*, 1996), were further enriched on equilibrium gradients (EGs). Figure 2C shows that in ISG fractions on the EG, a membrane-associated peak of VHS-GAT-GFP cofractionated with the ISG marker SgII. Note that most of the signal in EG fractions 1–4 can be attributed to soluble VHS-GAT-GFP (data not shown). Moreover, in Figure 2E, only very low amounts of VHS-GAT-GFP cofractionated with MSGs in fractions 10–12. The full-length GGA1-GFP was also found to be associated with SGs in the same way as the VHS-GAT-GFP (Figure 2B, D, and F). This finding is in accordance with the presence of ARF1, the GTPase that recruits GGAs to membranes (Boman *et al*, 2000), on ISGs (Austin *et al*, 2000). Retention of MPR in SGs, shown by its presence in ISGs and MSGs in VHS-GAT-GFP cells, as opposed to ISGs only in GGA1-GFP cells (Figure 2G), shows that the SG-associated VHS-GAT-GFP is also functional in binding MPR.

VHS-GAT-GFP has no effect on ISG formation but inhibits ISG membrane remodeling

Although our data in Figure 2 illustrate that SGs are present in VHS-GAT-GFP-expressing cells, it was also important to demonstrate directly that budding of regulated secretory cargo from the TGN is maintained in VHS-GAT-GFP-expressing cells. Therefore, we transfected PC12 cells with plasmids encoding VHS-GAT-GFP or GGA1-GFP, and obtained homogeneous VHS-GAT-GFP-positive and -negative and GGA1-GFP-positive cell populations by FACS. Sorted cell populations were reseeded, grown overnight, and subjected to a 5 min pulse with [^{35}S]-sulfate, followed by a 15 min chase with unlabeled sulfate. During the pulse, granins (CgB and SgII) and heparansulfate proteoglycan (hsPG) were sulfate-labeled in the TGN, and during the chase, these sulfated proteins were packaged into ISGs and constitutive secretory vesicles (CSVs), respectively, that bud from the TGN (Tooze and Huttner, 1990). VG fractionation of the PNS from both cell populations after 15 min of chase demonstrated that the sulfated proteins peaked in fractions 1–4, where both ISGs and CSVs fractionate (Tooze and Huttner, 1990) (Figure 3). Comparison of the sorted populations confirmed that budding from the TGN occurred in VHS-GAT-GFP- and GGA1-GFP-positive cells (Figure 3A and C), as well as in untransfected cells (Figure 3B). We have also demonstrated that constitutive (hsPG) and regulated (SgII) cargos are sorted into CSVs and ISGs in these cell populations (data not shown). These data show that TGN sorting of regulated and constitutive secretory proteins was unperturbed by VHS-GAT-GFP and GGA1-GFP expression.

We next examined the effect of VHS-GAT-GFP on the fate of components removed from the maturing granules, and on MSG membrane composition. In addition to MPR, a direct target of the GGAs, several transmembrane proteins are possible cargo in CCVs budding from maturing granules, including SNAREs such as VAMP4 (Eaton *et al*, 2000; Hinners *et al*, 2003) and Sx6 (Wendler *et al*, 2001), and SNARE partners such as synaptotagmin IV (Eaton *et al*, 2000), which are proposed to mediate ISG homotypic fusion. In the studies above, inclusion of cargo molecules in ISG-derived CCVs was deduced from their subcellular localization in ISGs and absence from MSGs. MSG localization of mutated cargos, unable to bind AP-1 (Hinners *et al*, 2003), was interpreted as inhibition of sorting into CCVs budding from ISGs, and consequent retention in MSGs. We followed the same rationale and assayed inhibition of budding from ISGs, using VAMP4 and Sx6 as putative cargo molecules. Cargo retention in SGs was analyzed in the neuroendocrine cell line AtT20 as well as in PC12 cells. We included AtT20 cells because in contrast to PC12 cells, where ISGs and MSGs do not display distinct spatial separation, MSGs in AtT20 cells localize to the tips of the cell processes. In AtT20 cells expressing VHS-GAT-GFP, both overexpressed VAMP4-Flag (Figure 4A) and endogenous Sx6 (Supplementary Figure 1A) colocalized at the tips with adrenocorticotropin hormone (ACTH). Such a colocalization was not found in cells expressing GGA1-GFP (Figure 4B and Supplementary Figure S1B). This finding suggested that both SNAREs failed to bud from ISGs in the VHS-GAT-GFP-expressing cells, and were therefore found in the ACTH-positive MSGs. In PC12 cells, to demonstrate retention of VAMP4-Flag in MSGs, we surmised that if the SNAREs are retained in SGs, their presence in granule-like structures not colocalizing with the TGN will increase. PC12 cells were cotransfected with VHS-GAT-GFP or GGA1-GFP, VAMP4-Flag, and the SG marker CgB-HA. CgB-HA was used here and in subsequent experiments to ensure that new SGs, formed in the presence of VHS-GAT-GFP or GGA1-GFP, are examined. As Figure 4C and D show for VAMP4-Flag, colocalization of these SNARE cargos with the granule marker CgB-HA is higher in VHS-GAT-GFP- than in GGA1-GFP-expressing cells. An identical result was obtained for Sx6 (Supplementary Figure S1C and D). The percentage of VAMP4-Flag and Sx6, which colocalizes with CgB-HA-positive granules outside of the TGN/juxtanuclear area, was quantified (Figure 4F and Supplementary Figure S1F) using the high-intensity signal of either VHS-GAT-GFP or GGA1-GFP to exclude the TGN. Immuno-EM double labeling of CgB-HA and VAMP4-Flag also demonstrated an increase in VAMP4-Flag in newly formed SGs in VHS-GAT-GFP-expressing cells (Figure 4G and H). Retention of endogenous VAMP4 in MSGs was also confirmed biochemically by showing that in metabolically labeled VHS-GAT-GFP cells, but not GGA1-GFP cells, VAMP4 could be immunoprecipitated from both MSG and ISG fractions (Figure 4E). We interpret the data above to suggest inhibition of ISG-derived CCV budding mediated by the VHS-GAT-GFP.

VHS-GAT-GFP does not affect homotypic fusion

Although the VHS-GAT-GFP caused retention of cargo (MPR, VAMP4, and Sx6) in the SGs that is normally removed throughout their maturation, theoretically, this retention could have been caused by inhibition of homotypic fusion, which would be predicted to inhibit generation of excess membrane available for CCV formation from the ISG. In order to exclude this, we tested if the fusion competence of ISGs

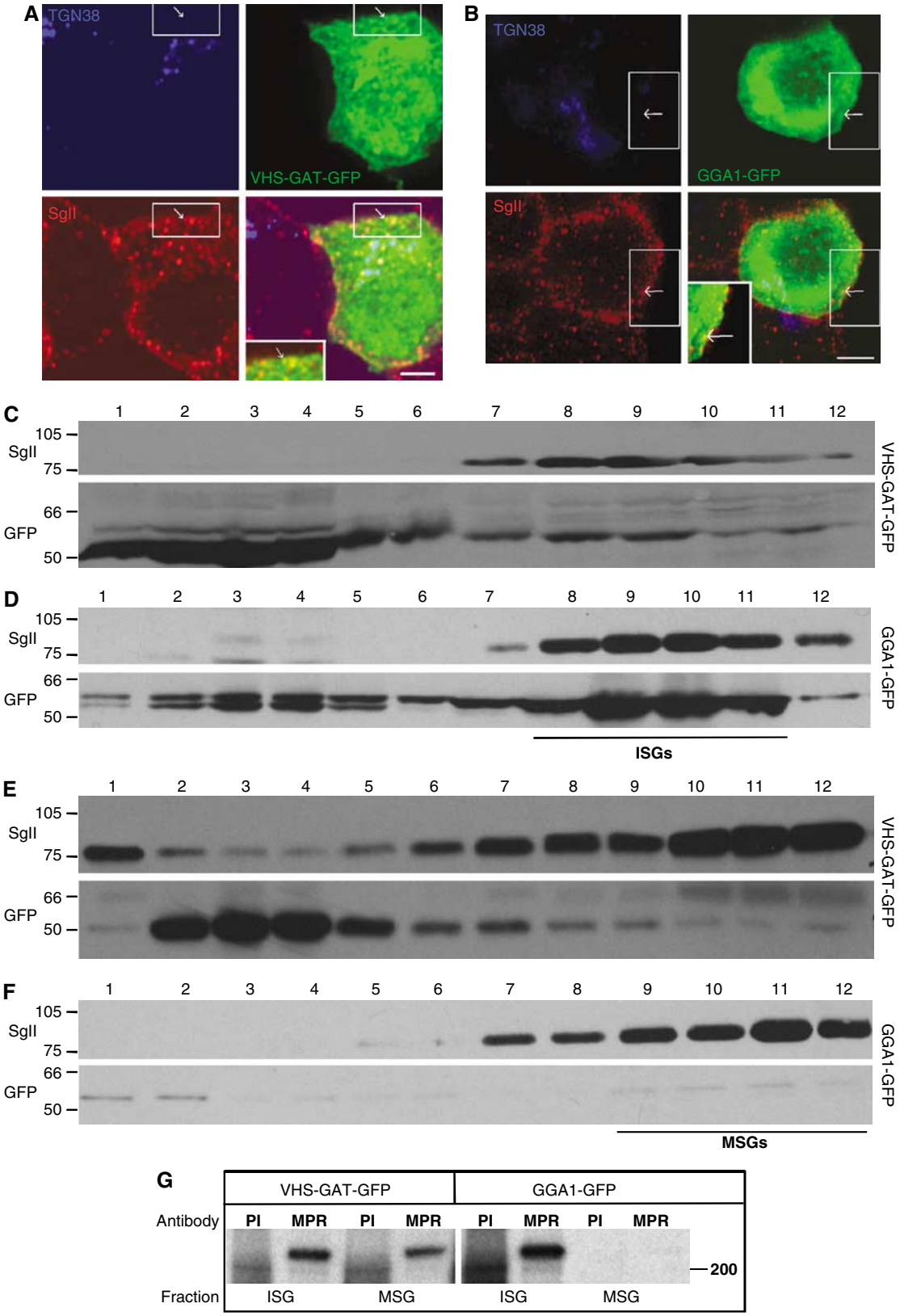

Figure 2 VHS-GAT-GFP is found on ISGs, and inhibits removal of MPR from ISGs. PC12 cells transfected with (**A**) VHS-GAT-GFP (green) or (**B**) GGA1-GFP (green) were fixed after 24 h and labeled with anti-TGN38 (blue) and anti-SgII (red) Abs and secondary Abs. Channel merges are shown in bottom right of each panel. Insets in the merged channels are the boxed region magnified. Arrows, GFP and SgII-positive, but TGN38-negative structures. Bar = 2 μm. (**C–F**) Fractions from EGs, which were loaded with (C, D) VG fractions 2–4, or (E, F) fractions 5–7 prepared from PNS of PC12 cells transfected with VHS-GAT-GFP (C, E) or GGA1-GFP (D, F). Proteins precipitated from the EG fractions were subjected to SDS–PAGE and immunoblotting using anti-SgII (upper panels) and anti-GFP (lower panels) Abs. Position of ISGs and MSGs on EGs is indicated. (**G**) ISG and MSG fractions prepared from [^{35}S]-Met/Cys-labeled FACS-sorted cells expressing VHS-GAT-GFP or GGA1-GFP were subjected to IP with anti-MPR ab, or a preimmune control (PI).

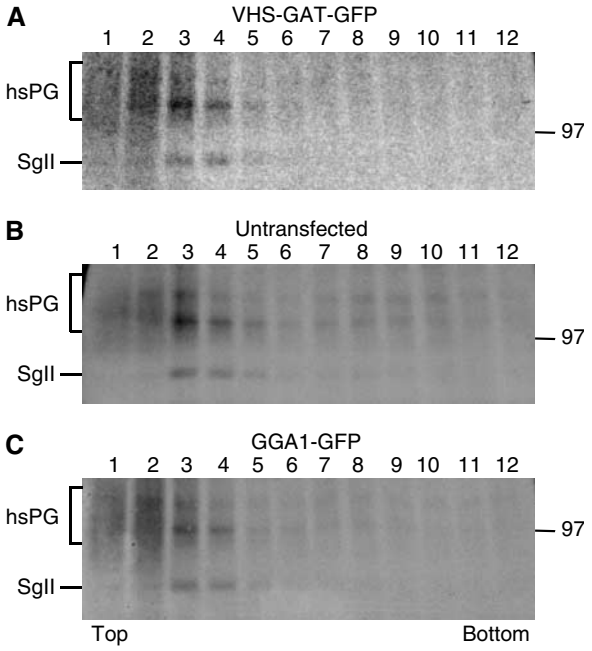

Figure 3 TGN budding of ISGs is not affected by VHS-GAT-GFP and GGA1-GFP. PC12 cells were transfected with either VHS-GAT-GFP or GGA1-GFP and 24 h later FACS-sorted. Cells positive for VHS-GAT-GFP (**A**), unstransfected (**B**), or positive for GGA1-GFP (**C**) were reseeded, cultured overnight, pulsed for 5 min with [^{35}S]-sulfate, and chased for 15 min to allow budding from the TGN. PNS was prepared from both cell populations and fractionated on a sucrose VG, and an aliquot of each fraction was subjected to SDS–PAGE and autoradiography. The peak of ISGs is found in fraction 3 and 4 under all conditions.

derived from VHS-GAT-GFP- and GGA1-GFP-expressing cells was compromised. We obtained VHS-GAT-GFP- and GGA1-GFP-positive PC12 cells by FACS sorting, and prepared a PNS from the sorted cells. The PNS derived from each of these populations was used in a new cell-free homotypic fusion assay. This new, more sensitive assay exploits dequenching of pyrenehexadecanoic acid (PHA)-labeled ISGs owing to a postfusion dilution of the dimer (excimer) form of the fluorophore, leading to an increase in the distinct monomeric fluorescence at 377 and 397 nm when excited at 330 nm. The increase in monomer fluorescence in the system used is not the result of translocation of labeled lipids to unlabeled membranes (Orsel *et al*, 1997; Struck *et al*, 1981). Figure 5A shows the emission spectra obtained from PHA-labeled ISGs before and after fusion. As predicted, the PHA monomer fluorescence at 377 and 397 nm has increased, which suggests that the PHA-labeled ISGs fused with the unlabeled ISGs, thus diluting and dequenching the PHA excimers. No excimer emission can be observed at the low PHA concentrations we used for our assays. The experiments illustrated in Figure 5B further validate the PHA fusion assay, as we are able to show that fusion rate is dependent on ATP, and inhibited by an Ab to the SNARE Sx6 shown to be involved in ISG–ISG fusion (Wendler *et al*, 2001). Cytosol-based PHA fusion assays have also shown that fusion rate is dependent on cytosol, and that the new assay recapitulates the specificity of fusion between ISGs and not between ISGs and MSGs (Urbé *et al*, 1998; P Sakya, S Tooze and B Larijani, in preparation). As shown in Figure 5C and D, the rate of fusion between ISGs and ISGs in the PNS prepared from VHS-GAT-GFP- or GGA1-GFP-positive cells was similar. This suggests that any effect of the VHS-GAT-GFP on ISG-derived cargo vesicle formation was not due to an effect on fusion, and thereby the availability of excess membrane, but rather a direct effect on budding.

SgII processing is inhibited in VHS-GAT-GFP-expressing cells

SgII is an abundant SG protein with several dibasic amino-acid cleavage sites; although in PC12 cells, which lack the appropriate prohormone convertases, it is not processed in the SGs. However, transfection of PC12 cells with the endopeptidase prohormone convertase 2 (PC2) leads to the processing of SgII to an 18 kDa form, p18 (Dittié and Tooze, 1995). p18 can be detected by a specific mAb, which does not recognize any of the p18 precursors (Urbé *et al*, 1998). We capitalized on this well-characterized intragranular processing and the p18 Ab in order to ask if SgII processing is affected by VHS-GAT-GFP expression. Flowcytometry analysis shows that in PC12 cells cotransfected and positive for PC2 and VHS-GAT-GFP, p18 was demonstrably reduced as compared to cells positive for PC2 and GGA1-GFP (Figure 6A). If the inhibition of SgII processing were genuine, it is also expected that full-length SgII would accumulate. This indeed was the case in the VHS-GAT-GFP- and PC2-positive subpopulation (Figure 6B). Furthermore, the positive correlation expected between the enzyme PC2 and its product p18 is abrogated in VHS-GAT-GFP-positive cells, as compared to GGA1-GFP-positive cells (Figure 6C). This last result predicts that PC2 activity is compromised, as the concentration of the product is not related to the concentration of the enzyme. The effect of VHS-GAT on p18 levels is specific as both the levels of an unrelated luminal Golgi protein (mannosidase II (Mann

Figure 4 VHS-GAT-GFP but not GGA1-GFP inhibits the removal of VAMP4 from maturing ISGs. (**A, B**) AtT20 cells were cotransfected with either (A) VHS-GAT-GFP or (B) GGA1-GFP and VAMP4-Flag and fixed 24 h post-transfection. Anti-Flag (red) and anti-ACTH (blue) were visualized with secondary Abs by confocal microscopy. GFP channel is shown in white. Arrow, ACTH and VAMP4-Flag colocalizing at cell tip. Bars = 5 μm. (**C, D**) PC12 cells were cotransfected with CgB-HA and VAMP4-Flag and either (C) VHS-GAT-GFP or (D) GGA1-GFP, and fixed 24 h post-transfection. Anti-HA (red) and anti-Flag (blue) Abs were visualized with secondary Abs by confocal microscopy. White channel, GFP. Arrows in (C), VAMP4-Flag positive granules. Bars = 1 μm. (**E**) A PNS from VHS-GAT-GFP and GGA1-GFP FACS sorted, [^{35}S]-Met/Cys-labeled cells was used to prepare ISG and MSG fractions. Membranes sedimented from these fractions were used for VAMP4 IP using a VAMP4 (V4) or an NR Ab. (**F**) Quantitation of the percentage of VAMP4-Flag structures colocalized with CgB-HA outside of the TGN/juxtanuclear area in PC12 cells transfected as in (C) (blue bar) and (D) (red bar). Percentage of VAMP4-Flag colocalization with CgB-HA was calculated based on the means of five independent observations, using the LSM 510 software. Student's *t*-test shows that the extent of colocalization is higher in the VHS-GAT-GFP-expressing cells than in cells expressing GGA1-GFP ($P \leqslant 1\%$). (**G**) Representative immuno-EM images of new granules positive for CgB-HA (10 nm gold, arrow) and VAMP4-Flag (5 nm gold, arrowhead). Images from VHS-GAT-GFP FACS-sorted cells are shown. (**H**) Quantitation of VAMP4-Flag-positive and -negative new granules in the two FACS-sorted populations. Fischer's exact test analysis shows the proportion of VAMP4-Flag-positive new granules in VHS-GAT-GFP cells is significantly higher than in GGA1-GFP cells ($P \leqslant 1\%$), $n = 3$. Bar = 100 nm.

II)) and PC2 were not changed in the VHS-GAT-GFP-positive cells (Figure 6D and E, respectively). PC2 sorting to new (CgB-HA-positive) SGs was also unaffected by VHS-GAT-GFP (Figure 6F and G).

When expressed in PC12 cells, the PC2 precursor, pro-PC2, is sorted into SGs (Dittié and Tooze, 1995), where its 75 kDa form is converted by autocatalytic cleavage into its mature 68 kDa form (Matthews *et al*, 1994). To test the effect of VHS-

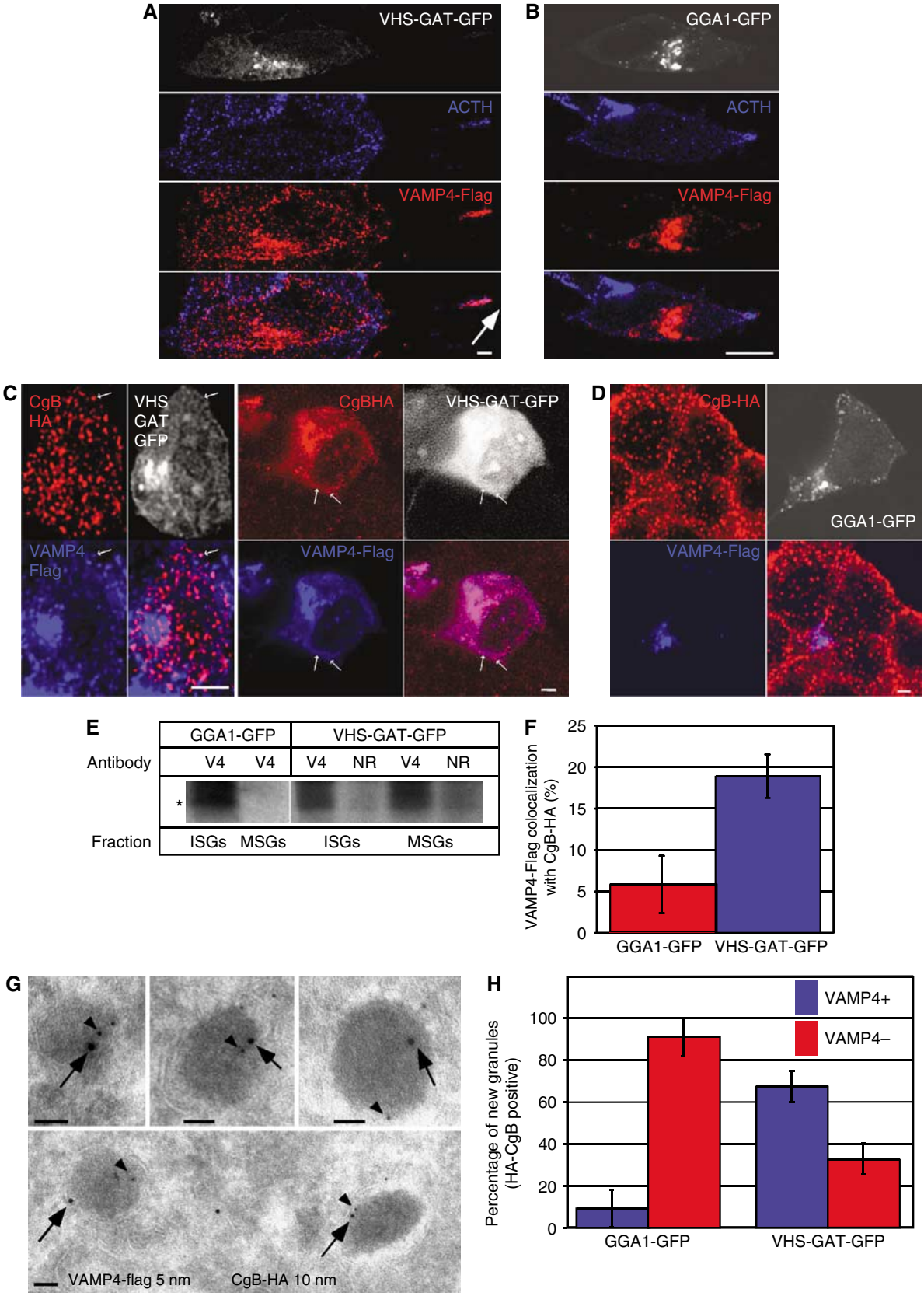

GAT-GFP on granule maturation, PC12 cells cotransfected with PC2 and VHS-GAT-GFP or GGA1-GFP were FACS sorted, lysed, and subjected to SDS–PAGE and immunoblotting using Abs against PC2 and p18. Even though PC2 sorting to new SGs was unaffected by the presence of VHS-GAT-GFP or GGA1-GFP (Figure 6F and G), PC2 autoconversion to the 68 kDa form was inhibited in VHS-GAT-GFP/PC2 compared to GGA1-GFP/PC2 cotransfected cells (Figure 6H). This inhibition was also concomitant with a reduction in the levels of SgII processing to p18 by PC2. Together, these data suggest that SG function, as measured by PC2 maturation and SgII processing, is inhibited by VHS-GAT-GFP.

GGA3 depletion by siRNA impairs SG maturation

In order to confirm the role of GGAs in SG maturation, in addition to overexpression of a DN GGA, we inhibited GGA function by siRNA-mediated knockdown of the GGA3, and monitored the effect of the knockdown on retention of VAMP4-Flag in SGs (see Figure 4), as well as on processing of transfected PC2 and endogenous SgII (see Figure 6) in PC12 cells. GGA3 was chosen as the siRNA target as we were restricted by the availability of reagents and information about the rat GGAs; importantly, as it was demonstrated that the GGAs act together in many cellular functions (Ghosh *et al*, 2003) and as GGA3 inhibition was found to be the most effective in downmodulating the other GGAs (Ghosh *et al*, 2003). Downregulation of GGA3 protein (Figure 7A) was corroborated by real-time RT–PCR analysis of mRNA levels (Figure 7B). To test the effect of GGA3 depletion on granule maturation, VAMP4-Flag colocalization with the marker for newly formed SGs, CgB-HA was analyzed by IF. As shown for the DN GGA1, granular localization of VAMP4-Flag (Figure 7D and E) was also increased when GGA function was compromised by depletion. PC2 and SgII processing were analyzed by FACS sorting and immunoblotting, as described above, and in agreement with these experiments, also showed that GGA3 depletion reduced PC2 and SgII processing to mature PC2 and p18, respectively (Figure 7F). Differences in the levels of GGA3 between the two-cell populations were confirmed during the FACS sorting, using GGA3 Abs. p18 was not assessed by flowcytometry (as in Figure 6) for lack of the appropriate Abs.

Discussion

Using a DN GGA construct, we have identified an inhibitor of the membrane remodeling events involved in SG maturation. Our assumption was that with such an inhibitor, we could assess the importance of these events in granule maturation. The inhibition of granule maturation by GGA3 depletion further corroborates our data from DN studies that GGAs play a role in granule maturation. This independent approach is important as the effects of GGA repression are also attained without the possible caveats associated with overexpression.

As the biological role of SGs is to ensure that mature, functional hormones are secreted from the cell, we also measure granule maturation by monitoring the fidelity of protein sorting, and the extent of intragranular processing. We found that ISGs still budded with properly sorted regulated SG cargo (i.e., SgII), and with an identical density to controls, in cells expressing VHS-GAT-GFP (Figure 3 and data not shown). These data support the view that budding of nascent granules from the TGN does not depend on clathrin coats (Arvan and Castle, 1998; Tooze, 1998). Indeed, EM data revealed that nascent granules budding from the TGN are only partially decorated with clathrin patches as opposed to nascent CCVs budding from the TGN, the PM, or even maturing ISGs (Orci *et al*, 1985; Tooze and Tooze, 1986).

Another consideration is the effect of the DN GGA on the previously reported requirement for ARF in ISG formation from the TGN. ISG formation was inhibited by treatment with brefeldin A (Rosa *et al*, 1992), an ARF-guanine nucleotide exchange factor inhibitor, and increased by the addition of N-terminal ARF peptides (Barr and Huttner, 1996). The lack of an effect by the DN GGA on ISG formation sustains the idea that pathways other than ARF-mediated coat recruitment are acting downstream of ARF during ISG formation. One candidate is the ARF effector, phospholipase D, which has been shown to stimulate granule formation (Chen *et al*, 1997).

Our data show that both the VHS-GAT-GFP and GGA1-GFP were localized to ISGs, whereas the VHS-GAT-GFP inhibited removal of cargo during SG maturation. These data support a role for GGAs in mediating CCV budding from maturing ISGs. Our results also show that MPR was not depleted from the forming SGs in VHS-GAT-GFP-expressing cells. We find very little VHS-GAT-GFP and GGA1-GFP on MSGs as might be anticipated owing to the absence of ARF-1 on MSGs (Austin *et al*, 2000), as GGAs are recruited to membranes by ARF (Dell'Angelica *et al*, 2000). We were unsuccessful in quantifying the VHS-GAT-GFP or GGA1-GFP present on ISG and MSGs membranes as both proteins dissociated from the membranes during the preparation of membrane fractions (data not shown).

ISGs belong to a growing family of intracellular vesicles, which bud from a large compartment and whose membrane is remodeled by coat-mediated secondary budding events. These include, for example, VTCs (vesicular tubular clusters), which mediate transport from the ER to the early Golgi, and are remodeled by COPI (Presley *et al*, 1997) and recently described GGA1, MPR, and clathrin-containing post-TGN tubular vesicular carriers (Puertollano *et al*, 2003). Finally, budding from the Glut4 donor compartment has been shown to be inhibited by VHS-GAT (Watson *et al*, 2004).

Another striking parallel between the Glut4 donor compartment and the ISGs is that cargo whose trafficking is inhibited by VHS-GAT may not interact directly with the GGA VHS binding site: both Glut4 (Watson *et al*, 2004) and VAMP4, as well as Sx6 (Figure 4 and Supplementary Figure S1), are retained in their respective compartment because of an effect of the VHS-GAT upstream of the compartment. Therefore, inhibition by DN GGA of cargo selection could be either a result of cargo interaction with AP-1, whose membrane off-rate constant is reduced by GGA (Puertollano *et al*, 2001b), or owing to its existence in a protein complex which is immobilized as a single entity (i.e., Sx6 which is in a complex with VAMP4; Wendler *et al*, 2001).

The domain of membrane on the ISG involved CCV formation could be present when the ISG buds, or is produced later if the SG core changes size (as may be the case for β-cells; Arvan and Castle, 1998). Alternatively, in PC12 cells,

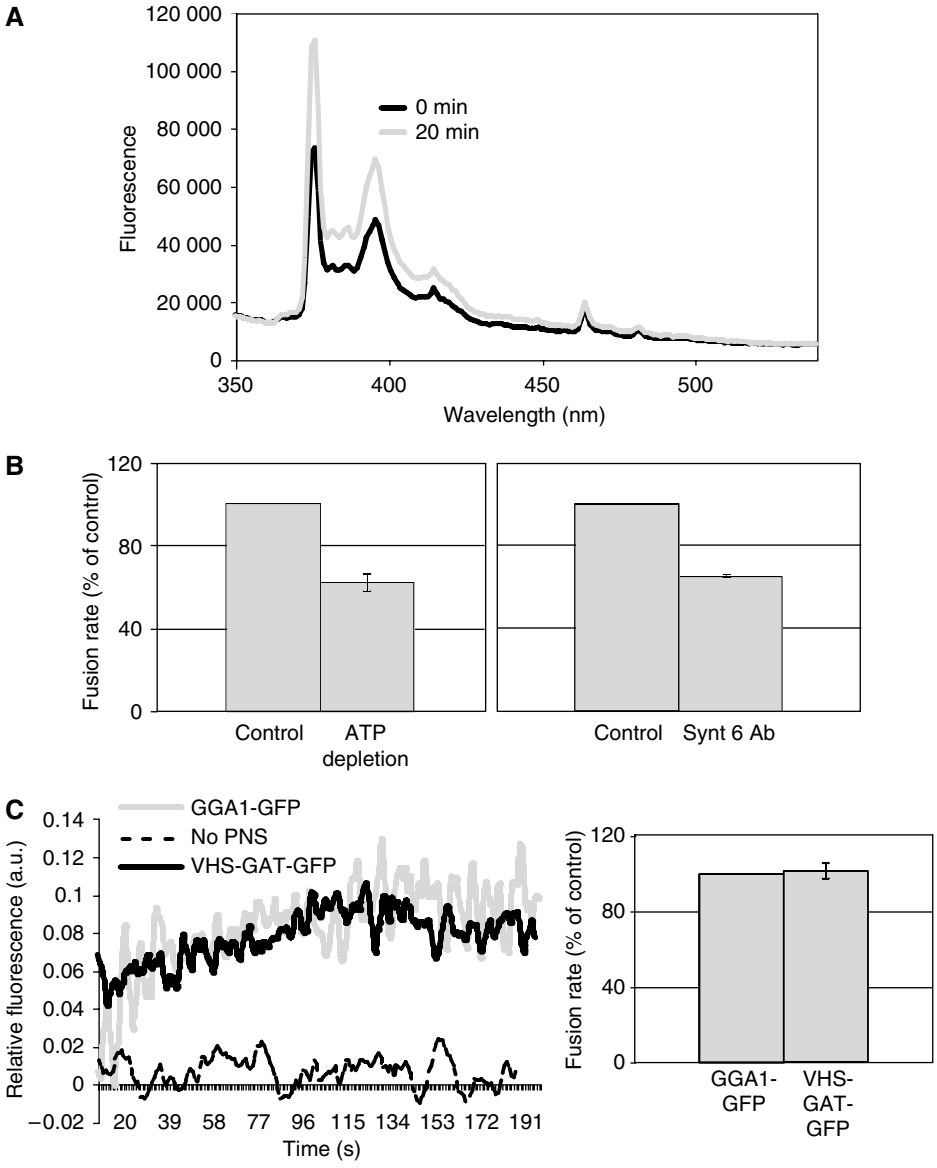

Figure 5 A PHA-based ISG–ISG fusion assay shows that ISG–ISG fusion rate is not affected by VHS-GAT-GFP or GGA1-GFP overexpression. (**A**) The emission spectrum of a mixture of PHA-labeled ISGs, PNS, ATP-regenerating system, and GTP in FB (standard fusion conditions) was measured at 0 min (black), and after 20 min incubation (gray) at 37°C. After incubation, the PHA monomer fluorescence intensity (peaks at 377 and 397 nm) has increased. (**B**) Rates of fusion measured by the initial slope of a time-based monitoring of fluorescence, as shown in (**C**). Left panel, PHA-labeled ISGs were preincubated for 5 min on ice with PNS under standard fusion conditions (control), or with 25 U hexokinase and 3.3 mM glucose (ATP depletion). Following the preincubation, fluorescence was monitored over time as described in Materials and methods, and initial slopes calculated. Right panel, PHA-labeled ISGs were preincubated 10 min on ice under standard fusion conditions (as in left panel), or with 27 μg/ml Sx6 Ab, before monitoring fluorescence ($n=3$). Both ATP depletion and Sx6 Ab treatments caused a significant reduction in the initial slopes of fluorescence over time, as confirmed by Student's *t*-tests ($P\leqslant 1\%$). (C) A fusion assay performed using PHA-labeled ISGs in fusion buffer containing GTP- and ATP-regenerating system (dashed line), or with a PNS from 10^7 FACS-sorted VHS-GAT-GFP-positive cells (black line), or 10^7 FACS-sorted GGA1-GFP positive cells (gray line). The fluorescence of PHA monomers (ex. 330, em. 377) was recorded continuously at 37°C. Data shown are normalized to infinite dilution of PHA obtained by adding 1% Triton X-100 to each condition after the signal had reached a plateau. Fusion rates (averages of three experiments) as in (B) are shown in the right panel ($n=3$).

it could be produced by homotypic fusion of ISGs during their maturation (Tooze, 1998). Regardless of the means by which CCV formation is promoted, it is likely that CCVs could pinch off only from the SG membrane once it has expanded to a critical surface area, which would allow sufficient membrane curvature required for CCV formation. It was therefore important to show that VHS-GAT, acting as a DN GGA, did not affect CCV formation via an effect on the extent of homotypic fusion. Such an effect would mean that VHS-GAT did not exert its effects by directly inhibiting coat formation. Although our data demonstrate that indeed coat recruitment and not homotypic fusion was perturbed, *a priori* it is not impossible that the GGAs could be involved in the regulation of homotypic fusion. Mattera *et al* and others (Mattera *et al*, 2003, 2004; Zhai *et al*, 2003) have shown that the GAE domain of GGA interacts with the rab4/rab5 effector complex, Rabaptin5–Rabex5. Acting either as a tether (Stenmark

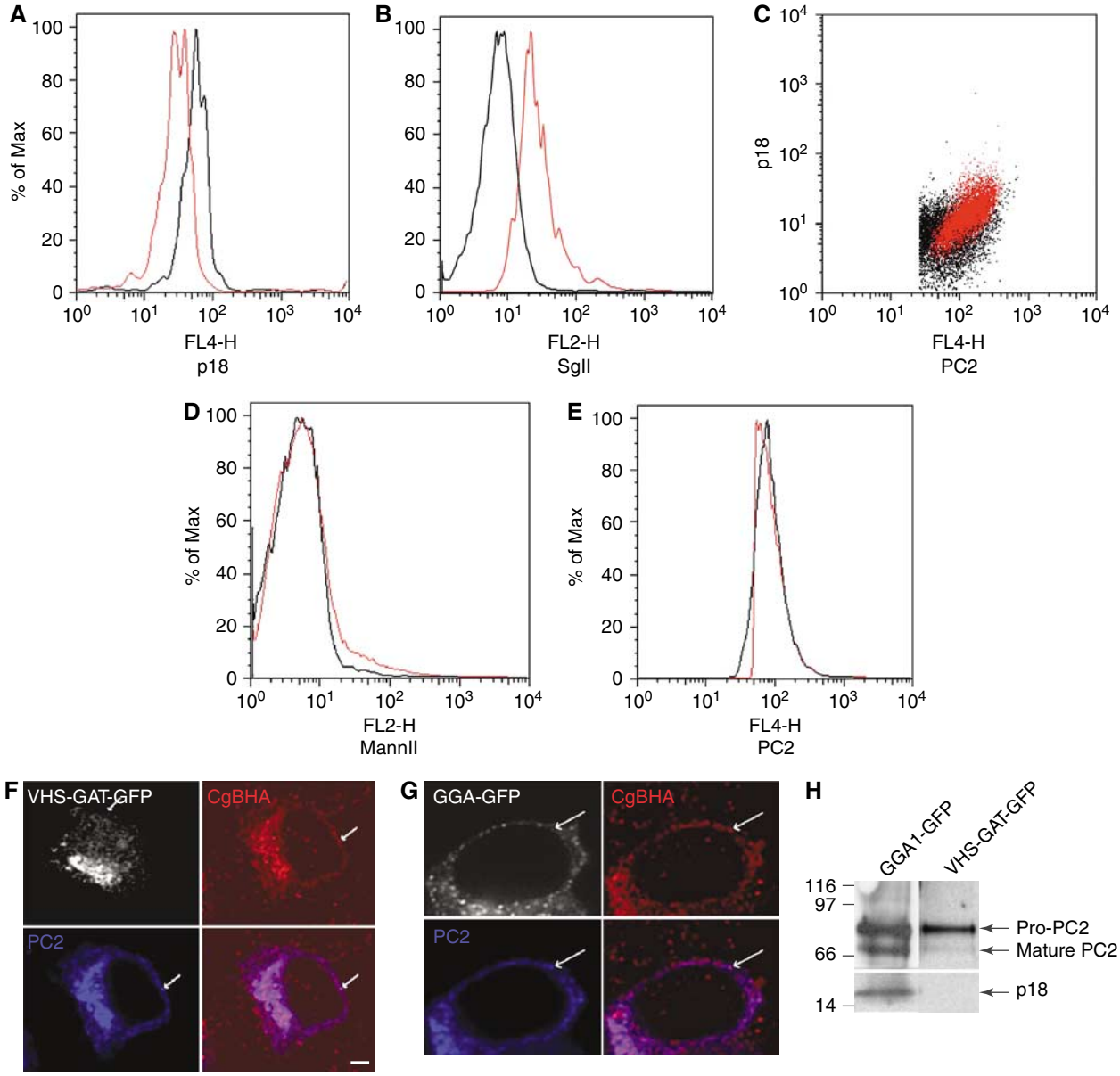

Figure 6 Inhibition of SgII processing in VHS-GAT-GFP- but not in GGA1-GFP-expressing cells. PC12 cells cotransfected with PC2 and either VHS-GAT-GFP (black lines in **A, B, D, E**), or as a negative control GGA1-GFP (red lines in A, B, D, E). At 24 h post–transfection, the cells were fixed and labeled with (A) and (**C**) anti-PC2 and anti-p18, (B) anti-SgII and anti-p18, (D) anti-PC2 and anti-Mann II, and (E) anti-PC2, and analyzed by flowcytometry with secondary Abs. Cells positive for either VHS-GAT-GFP (black) or GGA1-GFP (red) and PC2 (or p18 in B) were gated and analyzed for the distribution of p18 (A), SgII (B), MannII (D), and PC2 (E). Student's *t*-tests show that the ratios (median p18 in PC2-positive cells)/(median p18 in PC2-negative cells) in (A) and (median SgII in p18-positive cells)/(median SgII in p18-negative cells) in (B) are significantly (A) smaller ($P \leqslant 5\%$) or (B) larger ($P \leqslant 5\%$) in VHS-GAT-GFP- than in GGA1-GFP-positive cells. No significant difference was observed between the VHS-GAT-GFP and GGA1-GFP populations in (D) and (E). (C) Dot plots testing the correlation between p18 and PC2 levels in VHS-GAT-GFP- (black) and GGA1-GFP- (red) gated cells. One-way ANOVA shows that a significant ($P \leqslant 2.5\%$) linear trend exists between p18 and PC2 in GGA1-GFP-positive cells, but not in the VHS-GAT-GFP-positive cells. (**F**, **G**) PC12 cells were cotransfected with either VHS-GAT-GFP (F), or GGA1-GFP (G) and PC2 and fixed 24 h post-transfection. HA (red) and PC2 (blue) were visualized by confocal microscopy with secondary Abs, GFP channel (white). (**H**) PC12 cells cotransfected with PC2 and either GGA1-GFP (left lane), or VHS-GAT-GFP (right lane) were, after FACS sorting for GFP- and PC2-positive cells, lysed and subjected to SDS–PAGE and immunoblotting with anti-PC2 and anti-p18 Abs.

et al, 1995) or by displacing clathrin from GGA (Mattera *et al*, 2003), Rabaptin5–Rabex5 could in theory mediate GGA-dependent fusion. The lack of an effect of the VHS-GAT on ISG homotypic fusion suggests that the Rabaptin5–Rabex5 is either dispensable for ISG homotypic fusion or is involved in the process after recruitment to ISG membranes via an interaction with GGA-GAT or γ1 adaptin ear domain (Mattera *et al*, 2003).

Finally, our data show that blocking budding by VHS-GAT-GFP compromised processing of SgII in SGs. A similar observation was made by Kuliawat *et al* (2004) using an anchorless form of Sx6 to perturb membrane remodeling of granules in INS-1 β cells. Expression of this truncated Sx6 reduced insulin processing. Abrogation of the enzyme–product relationship between the endopeptidase PC2 and the SgII product p18 suggests that PC2 was malfunctioning in the

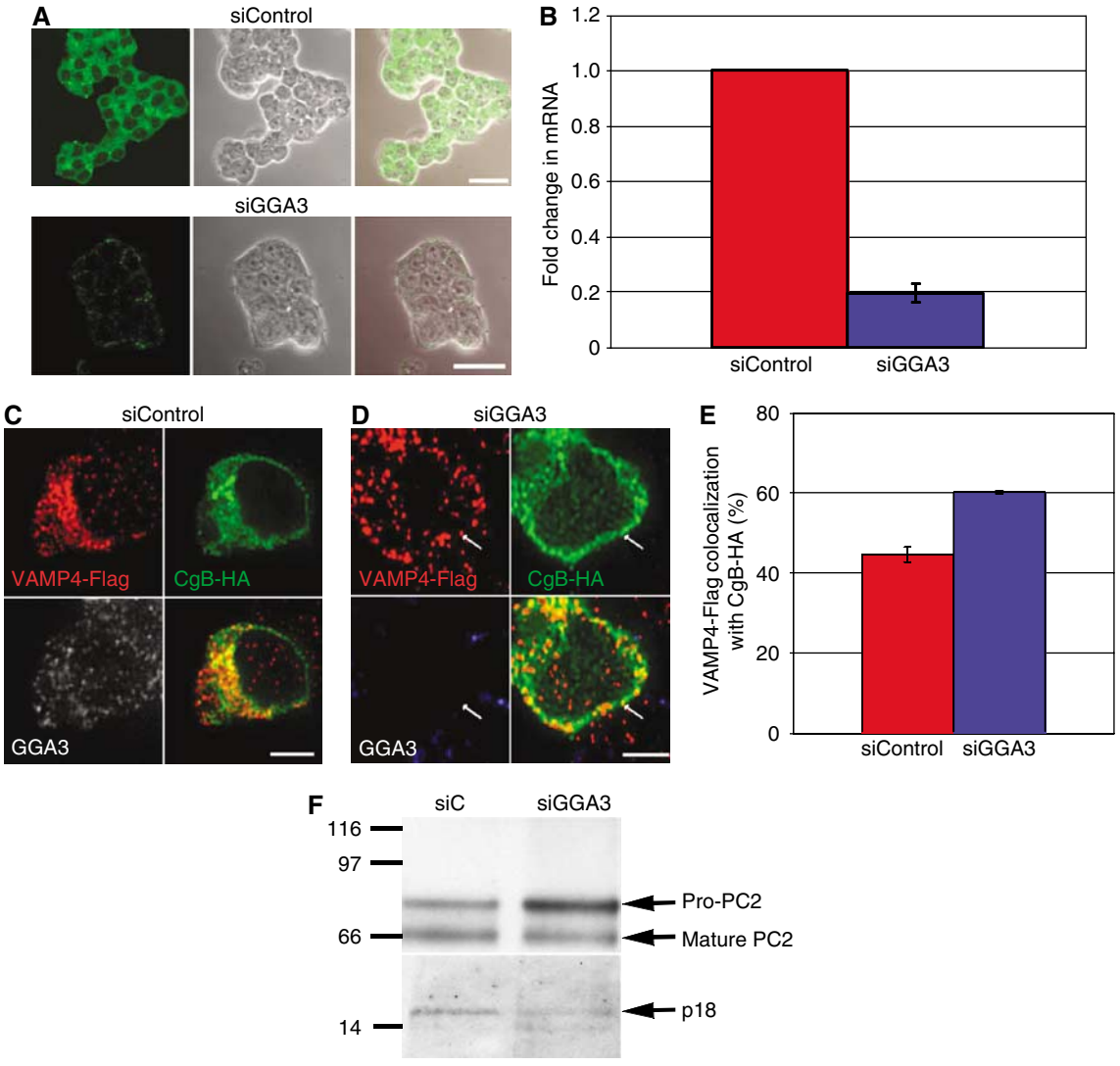

Figure 7 Depletion of GGA3 in PC12 cells inhibits VAMP4-Flag removal from maturing SGs and reduces pro-PC2 maturation. (**A**) PC12 cells were treated either with siControl (upper panel) or siGGA3 (lower panel), fixed, and labeled with anti-GGA3 Ab and secondary Ab (green). Representative confocal images, phase-contrast images, and channel merges are shown. Bar = 20 μm. (**B**) Real-time RT–PCR analysis of GGA3 mRNA in PC12 cells transfected with siControl or siRNA against GGA3 (siGGA3). (**C**–**E**) PC12 cells were transfected with siControl (C) or siGGA3 (D), and 48 h later, retransfected with the siRNAs, and with CgB-HA and VAMP4-Flag constructs, and fixed 24 h later. Anti-GGA3 (white), anti-HA (green), and anti-Flag (red) Abs were visualized with secondary Abs by confocal microscopy. (E) Quantitation of the percentage of all VAMP4-Flag structures colocalizing with CgB-HA, $n = 3$. Colocalization was quantified using the LSM software. Student's *t*-test shows that the extent of VAMP4-Flag colocalized with CgB-HA is significantly ($P \leqslant 5\%$) higher in siGGA3- than in siControl-treated cells. (**F**) PC12 cells were treated with siControl or siGGA3 and cotransfected with the PC2 plasmid. PC2-positive cells were FACS sorted from the siControl- and siGGA3-treated cell populations, and analyzed as in Figure 6F with PC2 and p18 Abs. The maturation of pro-PC2 to PC2 was inhibited in siGGA3-treated cells resulting in, on average, a 180% increase in the ratio (pro-PC2/mature PC2) in siGGA3- relative to siControl-treated cells. p18 levels were also reduced in siGGA3 cells by 30% on average.

granules of VHS-GAT-GFP-expressing cells. We propose that this malfunction is related to perturbation of the granule acidification machinery, which is probably necessary for PC2 maturation and processing and ensuing activation (Matthews *et al*, 1994). Our results indeed demonstrate an inhibition of PC2 processing in cells in which GGA function was inhibited. Current work is being carried out to monitor granule acidification in VHS-GAT-expressing cells using the pH-sensitive GFP, ratiometric pHluorin, fused to a granule marker. We speculate that the acidification of the MSGs (pH 5.5 as compared to 6.3 in ISGs; Urbé *et al*, 1997) is linked to ISG membrane remodeling in two ways: (1) retrieval of the excess membrane formed after ISG homotypic fusion (Urbé *et al*, 1998), which could increase the membrane density of the granule v-type H^+-ATPase and thus the acidification efficacy; (2) removal of proteins with potentially adverse effects on granule acidification such as Na^+/K^+-ATPase, which in theory might compete for ATP with the v-type H^+-ATPase, or, more likely, proton leaks (Wu *et al*, 2001). Comparative proteomics between ISGs and MSGs might reveal the identity of such candidates.

Materials and methods

Reagents and cells

All chemicals were from Sigma, except that ATP, GTP, creatine phosphate, and creatine phosphokinase were from Roche

(Germany) and [^{35}S]-sulfate and [^{35}S]-Met/Cys were from Amersham (UK). PC12 cells (clone 251) were grown in DMEM containing 10% horse serum, 5% FCS, and 20 mM glutamine. AtT20 cells were grown in DMEM containing 10% FCS and 4.5 gm/l glucose. Cells were transfected with Lipofectamine 2000 (Invitrogen, Carlsbad, CA) used as recommended.

Antibodies

Polyclonal anti-CI-MPR (STO52) (Dittié *et al*, 1999), anti-SgII (175) (Dittié and Tooze, 1995), anti-ACTH (Tooze and Tooze, 1986), and anti-p18mAb (Urbé *et al*, 1998) were used at a 1:1000 for indirect immunofluorescence (IF) and immunoblotting, and at a 1:100 for FACS. Polyclonal anti-PC2 Ab from Dr B Eipper (University of Connecticut, CT) was used at a 1:1000 for immunoblotting, and at a 1:100 for FACS. Polyclonal anti-GFP Ab (SG5) from Dr T Hunt (Cancer Research UK, London) was used at a dilution of 1:2000. MAb anti-Mann II from Dr G Warren (Yale University, CT) was used at 1:1000. Polyclonal anti-VAMP4 Ab (TG19) from Dr T Galli (Institut J Monod, Paris) was used for immunoprecipitation (IP). mAb anti-TGN38 (Affinity Bioreagents, CO), mAb anti-Sx6 (Transduction Laboratories, KY), mouse monoclonal (M2, Sigma) and chicken affinity-purified (ICL, OR) anti-Flag Abs and rat mAb anti-HA were used at a 1:1000 for IF and 1:100 for immuno-EM. mAb anti-GGA3 (Transduction Laboratories, KY) was used at 1:500 for IF, and at 1:50 for FACS. Secondary Abs, such as HRP-conjugated anti-mouse, and anti-rabbit IgGs (Amersham, UK), Alexa-555- and Alexa-647-conjugated anti-rabbit, anti-chicken and anti-mouse IgG (Molecular Probes, OR), and R-phycoerythrin-conjugated anti-mouse IgG (Dako, Denmark), were used as recommended.

Plasmids

VHS-GAT-GFP and GGA1-GFP plasmids were from Dr J. Bonifacino (NIH, MD). VAMP4-Flag plasmid was described previously (Hinners *et al*, 2003). pRC-PC2 was from Dr N Seidah (Clinical Research Institute of Montreal, Canada).

Indirect IF

At 24 h post–transfection, cells were fixed with 3% paraformaldehyde, permeabilized with 0.2% Triton X-100, stained with Abs (Dittié and Tooze, 1995), and analyzed by confocal microscopy using Zeiss LSM 510 and Huygens2 (for image deconvolution) softwares.

Fractionation of post-TGN vesicles and [^{35}S] labeling

A PNS from PC12 cells was subjected to fractionation on consecutive velocity and density sucrose gradients to prepare ISGs and MSGs, as described (Dittié *et al*, 1996). In brief, fractions 2–4 (ISGs) or 5–7 (MSGs) from the VG were loaded onto an EG. After centrifugation, fractions were acetone precipitated, and subjected to SDS–PAGE and immunoblotting. For the budding and IP assays, 2×10^7 FACS-sorted cells were reseeded in 15 cm dishes and grown overnight before [^{35}S]-sulfate pulse-chase (Tooze and Huttner, 1990) or overnight [^{35}S]-Met/Cys (IP) labeling. After adding 2.3×10^7 unlabeled cells to crack the cells more efficiently, a PNS was prepared, and fractionation was carried out as above. The fractions or samples from IP were subjected to SDS–PAGE and autoradiography with 2- to 3-week exposures.

Flowcytometry

Levels of p18, PC2, Mann II, and SgII in cells transfected with VHS-GAT-GFP or GGA1-GFP were determined using a Facscalibur flow cytometer (BDIS, CA). Cells in 10 cm dishes were transfected and harvested after 24 h. The cells were fixed, permeabilized for 3 min on ice with 0.2% Triton X-100, and stained with Abs. Fluorescence was detected in at least 10 000 cells, as determined by forward and side scatter criteria. Mo-Flo (Dako Cytomation, CO) and Aria (BDIS) cell sorters were used to sort cells. Exclusion of dead cells and cell aggregates was obtained using DAPI staining and pulse-width versus area measurements. Note the transfection efficiency of PC12 cells with plasmid DNA ranged between 10 and 30%.

Immunoprecipitation

VHS-GAT-GFP- and GGA1-GFP-transfected cells were FACS sorted and labeled overnight with 0.2 mCi [^{35}S]-Met/Cys. PNS from labeled cells was prepared and subjected to fractionation on consecutive VG and EG to obtain ISGs and MSGs. Membranes sedimented from 3 ml of ISGs or MSGs were used for VAMP4 IP using a VAMP4 (V4) or a nonrelevant (NR) Ab as described in Wendler *et al* (2001).

Immunoelectron microscopy

VHS-GAT-GFP and GGA1-GFP FACS-sorted cells were fixed in 4% paraformaldehyde and 0.2% glutaraldehyde in 0.1 M phosphate buffer and processed for cryoimmuno-EM as described (Liou *et al*, 1996). Immunogold double labeling and quantitation was carried out in a double-blind manner with anti-HA and anti-Flag Abs detected by protein A coupled to 10 and 5 nm gold, respectively. New (CgB-HA-positive) granules, made under overexpression of VHS-GAT-GFP or GGA1-GFP, were scored for VAMP4-Flag.

ISG–ISG fusion assay

Our novel PHA fluorescence-based fusion assay is based on established cell-free fusion assays: the content-mixing-based assay described by Urbé *et al* (1998), which reconstitutes fusion of purified ISGs, containing the endopeptidase PC2, with ISGs containing the [^{35}S]-sulfate-labeled substrate SgII, presents in a PNS. We could not use this assay because of the large number of cells required for a robust signal after IP, which we could not obtain in transfected and FACS-sorted PC12 cells. Our new assay is based on fusion of isolated ISGs with PNS, but capitalizes on fluorescence dequenching: PHA-labeled ISG membranes are incubated with unlabeled ISG membranes present in a PNS prepared from FACS-sorted cells. Upon fusion of the PHA-labeled membranes with unlabeled membranes, a reduction of PHA self-quenching is detected and measured as an increase in fluorescence (Orsel *et al*, 1997). Labeling of ISG membranes was carried out by metabolic incorporation of PHA (Molecular Probes, OR). The medium of confluent PC12 cells was replaced by medium containing 5 μg/ml PHA. Cells were incubated in the PHA-containing medium for 4 h at 37°C before harvesting, and ISGs were prepared as above. A measure of 28 μl of labeled ISGs were mixed with 100 μl of unlabeled PNS prepared from unsorted cells (Figure 4B) or from 6 to 8×10^6 FACS-sorted cells (Figure 4C), in a fusion buffer containing ATP-regenerating system and GTP as described in Urbé *et al* (1998). PHA fluorescence (ex. 330, em. 377) was measured continuously on a Quantamaster QM6/2003 fluorimeter (Photon Technology International, NJ) with thermostatted cuvette housing. All experiments were carried out at 37°C. The rate of fusion (Figure 4B) was taken to be the initial slope of the plot. Data were normalized to Triton X-100 (1%)-solubilized infinite dilution (maximal fluorescence) of PHA.

siRNA

siRNAs against rat GGA3 were designed and synthesized by Dharmacon (CO). Maximal knockdown was achieved with Dharmacon's mix of four duplexes (Smart pool) against rat GGA3 (XM_340935). Cells were transfected with 100 nM of either GGA3 siRNA pool or Dharmacon's nontargeting siControl (siC), using Dharmacon's Dharmafect2. siRNAs were replenished after 48 h and cells were assayed 24 h after the second transfection.

RT–PCR

Total RNA was purified from cells using RNeasy minikit (Qiagen, CA). cDNA was reverse transcribed using the Superscript II kit (Invitrogen, CA) and amplified using GGA3 primers (GTTCTCATCA GAGGCCGACAA; GCAGGATGTCCCCCAAACTAT) and GAPDH (normalizing control) primers (TGTCATCGTCACTGCACCTTC; GATGCAT TGCTGACAACGGT). mRNA was quantified using the Chromo 4 Real-Time PCR system (MJ Research, MA) and SYBR Green (Applied Biosystems, CA). Fold changes in mRNA levels were determined by the ratio of GAPDH-normalized amplicon numbers between GGA3 siRNA- and siC-treated cells.

Supplementary data

Supplementary data are available at *The EMBO Journal* Online.

Acknowledgements

We thank Derek Davis, Cathy Simpson, Gary Warnes, Ayad Eddaoudi, and Kirsty Allen from the FACS laboratory at Cancer Research UK for their valuable help with FACS of sorting the cells.

References

Arvan P, Castle D (1998) Sorting and storage during secretory granule biogenesis: looking backward and looking forward. *Biochem J* **332:** 593–610

Austin C, Hinners I, Tooze SA (2000) Direct and GTP-dependent interaction of ADP-ribosylation Factor 1 with clathrin adaptor protein AP-1 on immature secretory granules. *J Biol Chem* **275:** 21862–21869

Barr F, Huttner WB (1996) A role for ADP-ribosylation factor1, but not COP I, in secretory vesicle biogenesis from the *trans*-Golgi network. *FEBS Lett* **384:** 65–70

Boman AL, Zhang C, Zhu X, Kahn RA (2000) A family of ADP-ribosylation factor effectors that can alter membrane transport through the *trans*-Golgi. *Mol Biol Cell* **11:** 1241–1255

Bonifacino JS (2004) The GGA proteins: adaptors on the move. *Nat Rev Mol Cell Biol* **5:** 23–32

Chen YG, Siddhanta A, Austin CD, Hammond SM, Sung TC, Frohman MA, Morris AJ, Shields D (1997) Phospholipase D stimulates release of nascent secretory vesicles from the *trans*-Golgi network. *J Cell Biol* **138:** 495–504

Costaguta G, Stefan CJ, Bensen ES, Emr SD, Payne GS (2001) Yeast GGA coat proteins function with clathrin in Golgi to endosome transport. *Mol Biol Cell* **12:** 1885–1896

Dell'Angelica EC, Puertollano R, Mullins C, Aguilar RC, Vargas JD, Hartnell LM, Bonifacino JS (2000) GGAs: a family of ADP ribosylation factor-binding proteins related to adaptors and associated with the Golgi complex. *J Cell Biol* **149:** 81–94

Dittié AS, Tooze SA (1995) Characterisation of the endopeptidase PC2 activity towards SgII in stably transfected PC12 cells. *Biochem J* **310:** 777–787

Dittié AS, Hajibagheri N, Tooze SA (1996) The AP-1 adaptor complex binds to immature secretory granules from PC12 cells, and is regulated by ADP-ribosylation factor. *J Cell Biol* **132:** 523–536

Dittié AS, Klumperman J, Tooze SA (1999) Differential distribution of mannose-6-phosphate receptors and furin in immature secretory granules. *J Cell Sci* **112:** 3955–3966

Dittié AS, Thomas L, Thomas G, Tooze SA (1997) Interaction of furin in immature secretory granules from neuroendocrine cells with the AP-1 adaptor complex is modulated by casein kinase II phosphorylation. *EMBO J* **16:** 4859–4870

Doray B, Ghosh P, Griffith J, Geuze HJ, Kornfeld S (2002) Cooperation of GGAs and AP-1 in packaging MPRs at the *trans*-Golgi network. *Science* **297:** 1700–1703

Duncan MC, Costaguta G, Payne GS (2003) Yeast epsin-related proteins required for Golgi–endosome traffic define a gamma-adaptin ear-binding motif. *Nat Cell Biol* **5:** 77–81

Eaton BA, Haugwitz M, Lau D, Moore HP (2000) Biogenesis of regulated exocytotic carriers in neuroendocrine cells. *J Neurosci* **20:** 7334–7344

Ghosh P, Griffith J, Geuze HJ, Kornfeld S (2003) Mammalian GGAs act together to sort mannose 6-phosphate receptors. *J Cell Biol* **163:** 755–766

Ghosh P, Kornfeld S (2003) Phosphorylation-induced conformational changes regulate GGAs 1 and 3 function at the *trans*-Golgi network. *J Biol Chem* **278:** 14543–14549

Hinners I, Wendler F, Fei H, Thomas L, Thomas G, Tooze SA (2003) AP-1 recruitment to VAMP4 is modulated by phosphorylation-dependent binding of PACS-1. *EMBO Rep* **4:** 1182–1189

Hirsch DS, Stanley KT, Chen LX, Jacques KM, Puertollano R, Randazzo PA (2003) Arf regulates interaction of GGA with mannose-6-phosphate receptor. *Traffic* **4:** 26–35

Hirst J, Lui WWY, Bright NA, Totty N, Seaman MNJ, Robinson MS (2000) A family of proteins with gamma-adaptin and VHS domains that facilitate trafficking between the *trans*-Golgi network and the vacuole/lysosome. *J Cell Biol* **149:** 67–80

Jacques KM, Nie Z, Stauffer S, Hirsch DS, Chen L-X, Stanley KT, Randazzo PA (2002) Arf1 dissociates from the clathrin adaptor GGA prior to being inactivated by Arf GTPase-activating proteins. *J Biol Chem* **277:** 47235–47241

Klumperman J, Kuliawat R, Griffith JM, Geuze HJ, Arvan P (1998) Mannose 6-phosphate receptors are sorted from immature secretory granules via adaptor protein AP-1, clathrin, and syntaxin 6-positive vesicles. *J Cell Biol* **141:** 359–371

Kuliawat R, Kalinina E, Bock J, Fricker L, McGraw TE, Kim SR, Zhong J, Scheller R, Arvan P (2004) Syntaxin-6 SNARE involvement in secretory and endocytic pathways of cultured pancreatic beta-cells. *Mol Biol Cell* **15:** 1690–1701

Kuliawat R, Klumperman J, Ludwig T, Arvan P (1997) Differential sorting of lysosomal enzymes out of the regulated secretory pathway in pancreatic β-cells. *J Cell Biol* **137:** 595–608

Liou W, Geuze HJ, Slot JW (1996) Improving structure of cryosections for immunogold labeling. *Histochem Cell Biol* **106:** 41–58

Mattera R, Arighi CN, Lodge R, Zerial M, Bonifacino JS (2003) Divalent interaction of the GGAs with the Rabaptin-5–Rabex-5 complex. *EMBO J* **22:** 78–88

Mattera R, Puertollano R, Smith WJ, Bonifacino JS (2004) The trihelical bundle subdomain of the GGA proteins interacts with multiple partners through overlapping but distinct sites. *J Biol Chem* **279:** 31409–31418

Matthews G, Shennan KIJ, Seal AJ, Taylor NA, Colman A, Docherty K (1994) Autocatalytic maturation of the prohormone convertase PC2. *J Biol Chem* **269:** 588–592

McKay MM, Kahn RA (2004) Multiple phosphorylation events regulate the subcellular localization of GGA1. *Traffic* **5:** 102–116

Mullins C, Bonifacino JS (2001) Structural requirements for function of yeast GGAs in vacuolar protein sorting, alpha-factor maturation, and interactions with clathrin. *Mol Cell Biol* **21:** 7981–7994

Nielsen MS, Madsen P, Christensen EI, Nykjar A, Gliemann J, Kasper D, Pohlmann R, Petersen CM (2001) The sortilin cytoplasmic tail conveys Golgi–endosome transport and binds the VHS domain of the GGA2 sorting protein. *EMBO J* **20:** 2180–2190

Orci L, Ravazzola M, Amherdt M, Louvard D, Perrelet A (1985) Clathrin-immunoreactive sites in the Golgi apparatus are concentrated at the *trans* pole in polypeptide hormone-secreting cells. *Proc Natl Acad Sci USA* **82:** 5385–5389

Orsel JG, Bartoldus I, Stegmann T (1997) Kinetics of fusion between endoplasmic reticulum vesicles *in vitro*. *J Biol Chem* **272:** 3369–3375

Presley JF, Cole NB, Schroer TA, Hirschberg K, Zaal KJM, Lippincott-Schwartz J (1997) ER-to-Golgi transport visualized in living cells. *Nature* **389:** 81–85

Puertollano R, Bonifacino JS (2004) Interactions of GGA3 with the ubiquitin sorting machinery. *Nat Cell Biol* **6:** 244–251

Puertollano R, Aguilar RC, Gorshkova I, Crouch RJ, Bonifacino JS (2001a) Sorting of mannose 6-phosphate receptors mediated by the GGAs. *Science* **292:** 1712–1716

Puertollano R, Randazzo PA, Presley JF, Hartnell LM, Bonifacino JS (2001b) The GGAs promote ARF-dependent recruitment of clathrin to the TGN. *Cell* **105:** 93–102

Puertollano R, van der Wel NN, Greene LE, Eisenberg E, Peters PJ, Bonifacino JS (2003) Morphology and dynamics of clathrin/GGA1-coated carriers budding from the *trans*-Golgi network. *Mol Biol Cell* **14:** 1545–1557

Rosa P, Barr FA, Stinchcombe JC, Binacchi C, Huttner WB (1992) Brefeldin A inhibits the formation of constitutive secretory vesicles and immature secretory granules from the *trans*-Golgi network. *Eur J Cell Biol* **59:** 265–274

Shiba Y, Takatsu H, Shin HW, Nakayama K (2002) Gamma-adaptin interacts directly with Rabaptin-5 through its ear domain. *J Biochem (Tokyo)* **131:** 327–336

Stenmark H, Vitale G, Ullrich O, Zerial M (1995) Rabaptin-5 is a direct effector of the small GTPase rab5 in endocytic membrane fusion. *Cell* **83:** 423–432

Struck DK, Hoekstra D, Pagano RE (1981) Use of resonance energy transfer to monitor membrane fusion. *Biochemistry* **20:** 4093–4099

Tooze J, Tooze SA (1986) Clathrin-coated vesicular transport of secretory proteins during the formation of ACTH-containing secretory granules in AtT20 cells. *J Cell Biol* **103:** 839–850

Tooze SA (1998) Biogenesis of secretory granules in the *trans*-Golgi network of neuroendocrine and endocrine cells. *Biochim Biophys Acta* **1404:** 231–244

Tooze SA, Huttner WB (1990) Cell-free protein sorting to the regulated and constitutive secretory pathways. *Cell* **60:** 837–847

Urbé S, Dittié A, Tooze SA (1997) pH-dependent processing of secretogranin II by the endopeptidase PC2 in isolated immature secretory granules. *Biochem J* **321:** 65–74

Urbé S, Page LJ, Tooze SA (1998) Homotypic fusion of immature secretory granules during maturation in a cell-free assay. *J Cell Biol* **143:** 1831–1844

Varlamov O, Eng FJ, Novikova EG, Fricker LD (1999) Localization of metallocarboxypeptidase D in AtT-20 cells. Potential role in prohormone processing. *J Biol Chem* **274:** 14759–14767

Watson RT, Khan AH, Furukawa M, Hou JC, Li L, Kanzaki M, Okada S, Kandror KV, Pessin JE (2004) Entry of newly synthesized GLUT4 into the insulin-responsive storage compartment is GGA dependent. *EMBO J* **23:** 2059–2070

Wendler F, Page L, Urbé S, Tooze SA (2001) Homotypic fusion of immature secretory granules during maturation requires syntaxin 6. *Mol Biol Cell* **12:** 1699–1709

Wu MM, Grabe M, Adams S, Tsien RY, Moore HP, Machen TE (2001) Mechanisms of pH regulation in the regulated secretory pathway. *J Biol Chem* **276:** 33027–33035

Zhai P, He X, Liu J, Wakeham N, Zhu G, Li G, Tang J, Zhang XC (2003) The interaction of the human GGA1 GAT domain with rabaptin-5 is mediated by residues on its three-helix bundle. *Biochemistry* **42:** 13901–13908

Zhu Y, Doray B, Poussu A, Lehto VP, Kornfeld S (2001) Binding of GGA2 to the lysosomal enzyme sorting motif of the mannose-6-phosphate receptor. *Science* **292:** 1716–1718